# New measurements of the antineutrino–spin asymmetry in beta decay of the neutron and restriction for mass of $W_R$

I. A. Kuznetsov, A. P. Serebrov, I. V. Stepanenko, A. V. Aldushchenkov,
M. S. Lasakov, and A. A. Kokin
*Petersburg Nuclear Physics Institute, 188350 Gatchina, Russia*

Yu. A. Mostovoi
*Kurchatov Institute, 123182 Moscow, Russia*

B. G. Yerozolimsky
*Harvard University, Cambridge USA 02138*

M. S. Dewey
*National Institute of Standards and Technology, Gaithersburg, Maryland USA 20899*

(Submitted 28 July 1994)
Pis'ma Zh. Eksp. Teor. Fiz. **60**, No. 5, 311–316 (10 September 1994)

New results of measurements of neutron antineutrino–spin asymmetry coefficient $B$ in the beta decay of polarized neutrons are reported. This work was carried out on the polarized neutron vertical channel of the WWR-M reactor at PNPI (Gatchina). The value of the antineutrino spin asymmetry coefficient was obtained from the results of measurements of the experimental asymmetry, $x = BP = 0.6617 \pm 0.0044$, and from the results of measurements of the beam polarization, $P = (66.88 \pm 0.22)\%$: $B = 0.9894 \pm 0.0083$. This allows us to place restrictions on $M_{W_R}$: $M_{W_R} > 282$ GeV/c$^2$ (90% c.l.). © *1994 American Institute of Physics.*

Precise measurements of neutron beta decay parameters allow one to test the standard model of weak interactions. The accuracy of measurements of the neutron lifetime and electron–spin asymmetry has recently been improved considerably. This allows one to determine, with good accuracy, the vector and axial vector coupling constants of weak interactions. At the same time, the vector coupling constant $G_v$ obtained from neutron data is in poor agreement with $G_v$ obtained from superallowed nuclear $0^+ \to 0^+$ transitions.[1–3] Analysis of this discrepancy, together with the data from $^{19}$Ne in the framework of the left-right model of weak interactions, makes it possible to obtain the mass region of $W_R$ of 230 GeV/c$^2$ (Refs. 2 and 3). This result is in contradiction with the restrictions from muon decay and restrictions from direct searches for an additional vector boson $W'$ (Refs. 4 and 5). Confirmation of this restriction directly from antineutrino–spin asymmetry of neutron beta decay seems possible at a measuring accuracy better than 1% (Ref. 3).

This work was carried out at the vertical channel of polarized cold neutrons at the WWR-M reactor. The neutron capture flux density is $6 \times 10^8$ n/cm$^2$/sec. The maximum wavelength in the spectrum is 4.2 Å.

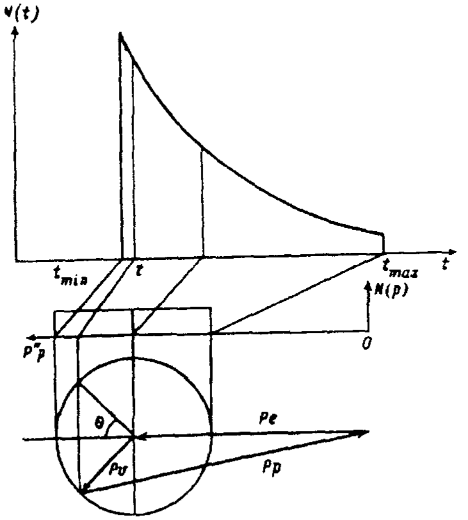

FIG. 1. The momentum diagram of neutron decay products and time-of-flight spectrum of protons for the ideal conditions.

The scheme of the measurement, proposed in Ref. 6, has now been adequately improved. Measurements of the momentum and angle of escape of the undetected antineutrino are possible because of the detection of the coincidence of the electron and the recoil proton, and because of the determination of their momenta. A kinematic diagram of beta decay is shown in Fig. 1. From the well-known energy of the decay and from measurement of the electron energy, the energy taken by the antineutrino can be calculated with an accuracy better than 0.75 keV, which is the maximum proton recoil energy. For a known electron momentum, all possible values of the antineutrino momentum lie on a sphere of radius $P_{\bar\nu}=(E_0-E_e)/c$, where $P_{\bar\nu}$ is the antineutrino momentum, $E_0$ is the total kinematic energy of decay, and $E_e$ is the electron energy. The measurement of the parallel projection of the proton momentum with respect to the electron momentum allows us to determine the antineutrino escape angle and, as a result, to reconstruct the beta decay event. The value of $P^{\parallel}_p$ can be determined by the time-of-flight method.

The events detected in this experiment can be written in the form of a coincidence matrix with the coordinates $E_e$ and $t_p$ for two opposite directions of the beam polarization. The count rate of events for each cell of this matrix can be calculated taking into account the Fermi function $f(E)$ and the correlation coefficients of the beta decay:

$$N^{\pm}_{ik}=f_i(E)\left[1+a\,\frac{v_i}{c}(\cos\,\theta_{e\bar\nu})_{ik}\pm PA\,\frac{v_i}{c}\cdot(\cos\,\theta_{\sigma e})_{ik}\pm PB(\cos\,\theta_{\sigma\bar\nu})_{ik}\right]. \tag{1}$$

This yields the experimental asymmetry

$$X_{ik}\equiv\frac{N^{+}_{ik}-N^{-}_{ik}}{N^{+}_{ik}+N^{-}_{ik}}=\frac{PA\,\frac{v_i}{c}(\cos\,\theta_{\sigma e})_{ik}+PB(\cos\,\theta_{e\bar\nu})_{ik}}{1+a\,\frac{v_i}{c}(\cos\,\theta_{e\bar\nu})_{ik}}, \tag{2}$$

and finally

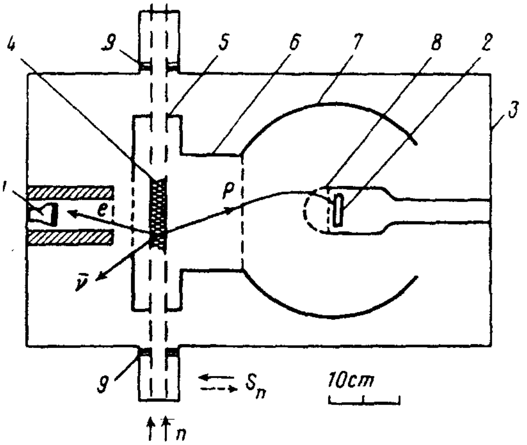

FIG. 2. Experimental setup. *1*—Electron detector; *2*—proton detector; *3*—chamber; *4*—decay region; *5*—cylindrical electrode; *6*—TOF cylinder; *7*—spherical electrode; *8*—spherical grid; *9*—LiF diaphragm.

$$PB=\frac{\left[X_{ik}\left(1+a\,\frac{v_i}{c}(\cos\,\theta_{e\bar{\nu}})_{ik}\right)\right]-AP\,\frac{v_i}{c}(\cos\,\theta_{\sigma e})_{ik}}{(\cos\,\theta_{\sigma\bar{\nu}})_{ik}},\qquad(3)$$

where $a$, $A$, and $B$ are the coefficients of the electron–antineutrino, electron–spin, and antineutrino–spin asymmetries, and $P$ is the degree of neutron polarization. The subscripts $i$ and $k$ correspond to a definite interval of the electron energy, $E_i$, and to a definite interval of the time of flight of a proton, $t_k$. For determination of $B$ it is necessary to know the beam polarization and the calculated values of $(v/c)\cos\,\theta_{e\bar{\nu}}$, $(v/c)\cos\,\theta_{\sigma e}$, and $\cos\,\theta_{\sigma\bar{\nu}}$. The values of the correlation coefficients $a$ and $A$ can be obtained from previous experiments.[7,8] It should be noted that the terms with the coefficients $a$ and $A$ are small ($<0.1$), and thus their errors are not important for the total error of $PB$.

A necessary part of this measurement is the correct calculation of mean cosine values: $(v/c)\cos\,\theta_{e\bar{\nu}}$, $(v/c)\cos\,\theta_{\sigma e}$, and $\cos\,\theta_{\sigma\bar{\nu}}$. To calculate these values we constructed a special Monte-Carlo model of the beta decay inside the apparatus. This model includes all the necessary geometrical parameters of the chamber, responses of the electron and proton detectors, distribution of neutron intensity inside the beam (this was measured in a separate experiment), shape of the electron spectrum in the form of the Fermi function, and characteristics of the amplitude-to-digital (ADC) and time-to-digital (TDC) converters. The real distribution of the electric field inside the apparatus was taken into account.

The schematic diagram of the installation is shown in Fig. 2. The decay region *4* is defined by means of a special diaphragm in front of the electron detector. The coincidences of signals of the electron *1* and the proton *2* detectors, which are located on each side of the decay region, are registered with opposite directions of the neutron polarization. The electron detector *1* is a photomultiplier with a plastic scintillator (diameter 75 mm and thickness 3 mm). The characteristics of this detector—energy resolution and fraction of backscattering of electrons—were determined in Ref. 8 by means of a magnetic beta spectrometer.

Decay protons which pass through the time-of-flight cylinder *6* their initial velocities are later accelerated and focused onto the detector *2* by an electric field with a potential of 25.6 kV applied between a spherical electrode *7* and spherical grid *8*. The proton detector is the assembly of two microchannel plates. The diameter of the detector is 65 mm. The detector allowed us to determine the time of flight of each proton with an accuracy of 10 nsec.

The entire chamber is surrounded with three pairs of current-carrying frames for compensation of the earth's magnetic field and to provide a guiding 0.5-Oe magnetic field in the chamber. The residual earth's field is not higher than 0.01 Oe. The changing of polarization direction is produced by a radio frequency (rf) flipper. To obtain an additional symmetrization of the measurements, we changed periodically the guiding magnetic field of the apparatus, together with the magnetic field of the flipper.

The data acquisition system was set up in the following way. The signal from the electron detector starts the proton time-of-flight measurements and at he same time is used for measuring the electron energy with help of ADC. The proton signal stops the time-of-flight measurements with help of TDC. For exact determination of the background, we used the method of delayed coincidence, and the measurement of the background was carried out simultaneously with the measurement of the coincidence signal, using the same electronic scheme.

The total data acquisition time was about 93 hours. The total number of decay events was 393 057. The signal-to-noise ratio in the area under the time-of-flight spectrum was 1.5:1.

The energy detector was calibrated at the beginning and end of each run. This was done to correct for possible gain shifts of the photomultiplier. Calibrations were carried out with the help of calibrated electron sources $^{113}$Sn and $^{137}$Cs.

Comparisons of the experimental results and calculations for the time and energy spectra are shown in Figs. 3a and 3b. The time-of-flight proton spectrum is integrated over energy and polarization states, while the energy spectrum is integrated over time and polarization states. We see that the agreement between experimental and calculated time-of-flight spectra is very good, and $\chi^2=1.15$. The agreement of the energy spectra in the low-energy region is poor. Analysis of the experimental data shows, however, that this does not influence the final result.

For treatment of the experimental data it is rather important that the theoretical and experimental time-of-flight spectra for each energy coincide. A special procedure of the analysis was followed to remove the effects of possible nonlinear discrepancy and possible shift between experimental and calculated time scales. For this purpose the time spectra were divided into a number of parts with equal intensity. In this case, each part of the spectra corresponds to a definite mean value of the cosines. This method allowed us to obtain a dependence of $B$ on $\cos\theta_{\sigma\tilde{\nu}}$ and to completely exclude the problem of the shift and nonlinear discrepancy of the time scales.

The results of treatment of experimental data in the form of a dependence of constant $PB$ on $\cos\theta_{\sigma\tilde{\nu}}$ are shown in Fig. 4. The average values are $PB=0.6617\pm0.0044$ and $\chi^2=0.78$.

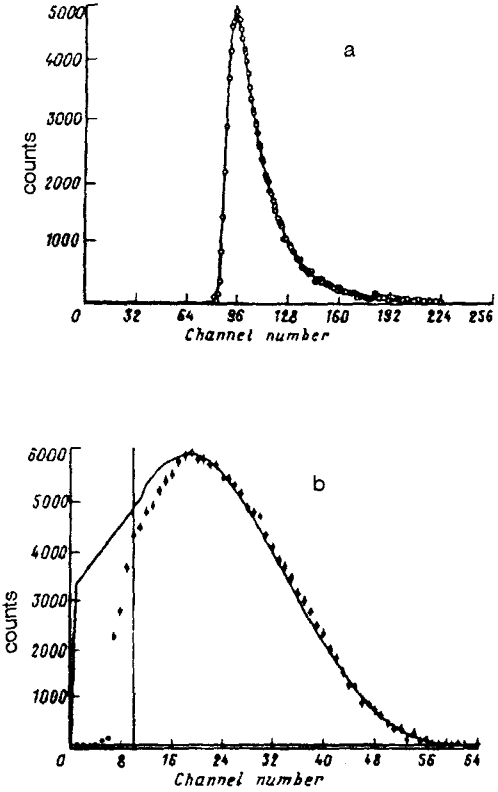

FIG. 3. Comparison of the experimental and simulation spectra. a—Time-of-flight spectra (1 channel corresponds to 10 nsec); b—energy spectra (1 channel is 10.75 keV, low threshold—10 channels correspond to 268 keV), ——— —computer simulation, O—experiment.

Analysis of possible systematic errors of this experiment was done by the method of variation of the model parameters in the frame of the uncertainty of these parameters. These parameters are the resolution of the electron detector, size of the energy channel, placement of zero in the energy scale, the value of the backscattering tail, and geometrical sizes and uncertainties in the knowledge of the correlation coefficients $a$ and $A$. This

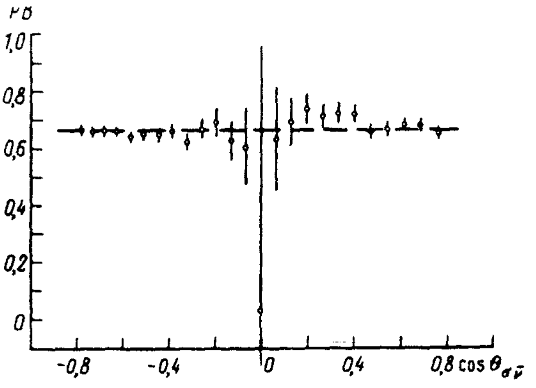

FIG. 4. Dependence of $B$ on $\cos\theta_{\sigma\bar{\nu}}$. The average values are $PB=0.6617\pm0.0044$ and $\chi^2=0.78$.

analysis gives us an estimate of the possible systematic error of our result: ±0.0037. The main part of this error deals with the low resolution of the electron detector.

The polarization of the neutron beam was measured by a new method of precise determination of the beam polarization. This method and its result are described in detail in Ref. 9. In these measurements, the behavior of the spectral space and angular distribution of the beam are taken into account. The polarization was averaged with the spectrum of the time of flight through the installation. The spectral dependence of the flipper efficiency was also taken into account. The measurements of polarization were carried out simultaneously with the measurement of $B$. As a result of these measurements, we obtained the following value of the polarization:

$$P=0.6688\pm0.0022.$$

Using the values of $PB$ and $P$, we obtained the following value of the antineutrino–spin asymmetry:

$$B=0.9894\pm0.0083.$$

The accuracy of this result is 4.2 times better than that of the previous measurement.[10]

Using this result, we can determine the restriction on the mass of the $W_R$ from the neutron $\beta$ decay. The antineutrino–spin asymmetry is not sensitive to the effect of the strong interactions, of the renormalization of the axial vector constant, and of the radiative corrections. Despite the discrepancy in the determination of the $\lambda$ ratio from different experiments, the values of $B$ are predicted, in the frame of the $V-A$ theory, to 0.988 with accuracy of 0.001. On the basis of the left-right model (at zero mixing angle) the value $B=(1-2\delta^2)B_V$–$A$, where $\delta$ is the squared ratio of the left and right boson masses. Because the deviation of the predicted and measured values is not within the accuracy of 0.0083, the restriction for $M_{W_R}$ amounts to 282 GeV/$c^2$ (90% c.l.). A more complete analysis of the restriction from this experiment is given on the plane squared mass ratio ($\delta$) and mixing angle ($\zeta$) (see Fig. 5). The experimental data for the neutron lifetime, the neutron–electron spin asymmetry, lifetime of the $0^+\rightarrow0^+$ transitions, and lifetime and asymmetry of $^{19}$Ne, which demonstrate the origin of the mass of about 230 GeV/$c^2$, are analyzed in Fig. 5. The results of our experiment fail to confirm the existence of this island directly from the neutron beta decay.

The potential of this method is not fully realized here, because the collection time of the statistics was only 93 hours. Since the systematic errors are not observed in this experiment, the experiment can be improved by prolongation of the collection of statistics. Apparently, the restriction of the statistical accuracy in this experiment should be estimated at the level of 0.2%. This accuracy is comparable with the accuracy of the determination of polarization. However, as was mentioned in Ref. 9, the accuracy of polarization can be improved to 0.1% by using supermirrors to polarize the beam. The systematic error can be decreased by using an electron detector with a high energy resolution.

The future prospects of this experiment, which were mentioned above, allow us to discuss the extension of this limit to 500 GeV/$c^2$.

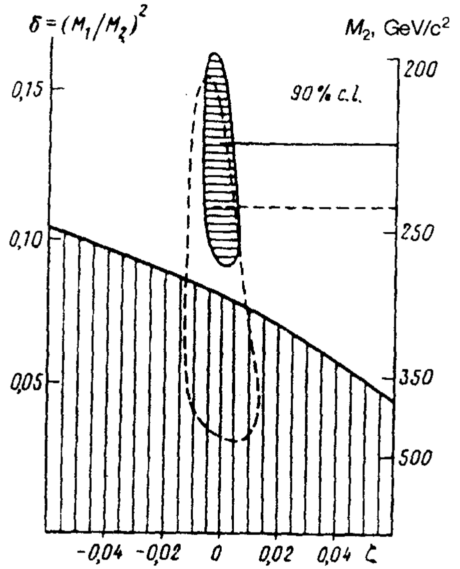

FIG. 5. The restriction for the left-right model from different experimental data. The horizontal shaded region—from the neutron $\beta$ decay, nuclear $0^+ \to 0^+$ transitions and from the decay of the $^{19}$Ne (the region shown by the dotted line—the same without data from Ref. 8). The restriction from the present measurement—the vertical shaded region.

This work was partially supported by ISF Grant No. 59000 and Grant No. 93-02-14382 of the Russian Fund for Fundamental Research.

[1] D. Dubbers *et al.*, Europhys. Lett. **11**, 195 (1990).
[2] A. S Carnoy *et al.*, Phys. Rev. Lett. **65**, 3249 (1991).
[3] A. P. Serebrov and N. V Romanenko, JETP Lett. **55**, 503 (1992).
[4] A. Jodido *et al.*, Phys. Rev. D **34**, 1967 (1986).
[5] F. Abe *et al.*, Phys. Rev. Lett. **67**, 2609 (1991).
[6] B. G. Erozolimsky *et al.*, Preprint IAE **3180** (1979), Russia.
[7] C. Stratova *et al.*, Phys. Rev. D **18**, 3970 (1978).
[8] B. G. Erozolimsky *et al.*, Yad. Fiz. **52**, 1583 (1990) [Sov. J. Nucl. Phys. **52**, 99 (1990)]; Preprint LNPI **1713** (1991), Russia.
[9] A. P. Serebrov *et al.*, *New Method for Precise Determination of Neutron Beam Polarization* (to be published).
[10] B. G. Erozolimsky *et al.*, Yad. Fiz. **12**, 323 (1970) [**12**, 167 (1970)].

Published in English in the original Russian journal. Reproduced here with stylistic changes by the Translation Editor.